PERGAMON

International Journal of Solids and Structures 38 (2001) 7875–7884

INTERNATIONAL JOURNAL OF SOLIDS and STRUCTURES

www.elsevier.com/locate/ijsolstr

Shaking table tests of two shallow reticulated shells

Li Zhongxue [a,*], Shen Zuyan [b]

[a] *Department of Civil Engineering, Zhejiang University, Hangzhou 310027, China*
[b] *College of Civil Engineering, Tongji University, Shanghai 200092, China*

Received 12 September 2000; in revised form 16 March 2001

Abstract

In this paper, shaking table tests of two shallow reticulated shells under earthquake loading were described. Local and global dynamic instabilities were observed in the test and time–history curves for stresses of members and nodal displacements were given respectively. It was shown that there were sudden changes in these curves, which were regarded as the signs of local and global dynamic instability. Based on test results, the law of structural dynamic instability was summarized, the definition of dynamic instability and several practical criteria proposed by the authors were illuminated. Finally, some calculation results from theoretical analyses of the two models under static and dynamic loading were given. By comparison of them, it can be seen that there are many common properties that reflect the stability behaviors and can be used to determine the state of static and dynamic stability of structures.

Keywords: Reticulated shell; Shaking table test; Dynamic stability; Criterion for instability; Time–history curve; Earthquake loading

1. Introduction

Stability analysis is the most intricate and important problems in designing reticulated shells (Gioncu, 1995), which relates to numerous factors, such as the size and shape of imperfections (Morris, 1991), the real rigidity of joints (Lightfoot and Le Messurier, 1974; Oda, 1986), the elasto-plastic behavior of members (Blandford, 1996, 1997), the distribution of residual stresses near the ends of members (Ikeda and Mahin, 1984; Soroushian and Alawa, 1990) etc. Since determining these factors exactly is rather difficult, it is essential to carry out model tests for getting the real data about the stability of reticulated shells so as to disclose the law of structural dynamic instability. Many tests on static stability were carried out, such as Fathelbab (1987), Hatzis (1987), Meek and Loganathan (1989) and Li (1998). But few literatures regarding nonlinear dynamic stability of reticulated shells under earthquake loading can be found. It is possible that the structures lose stability under high level vertical earthquake motions, which is characterized by a sudden collapse and a sharp increase of the maximum deflection. This always results in losing serviceable function of structures and great disaster of economy and lives inevitably. Although the related research works were

* Corresponding author. Tel.: +86-571-795-2259; fax: +86-571-795-2165.
E-mail address: lizx@civil.zju.edu.cn (L. Zhongxue).

0020-7683/01/$ - see front matter
PII: S0020-7683(01)00075-0

performed recently by Ye (1995), Kato and Mukaiyama (1995), Kato et al. (1997), Ishikawa and Kato (1997) and Kim et al. (1997), there is little satisfying progress in this field.

Using the improved tracing technique of equilibrium path for static nonlinear stability, the authors have successfully traced the structural dynamic buckling and post-buckling equilibrium path, and obtained many valuable conclusions (Li, 1998). In this paper, shaken table tests of two shallow reticulated shell models were conducted, and the data from the tests were analyzed to verify the conclusions.

2. Purpose of the test

Based on the theoretical analysis, the definition of elastic geometrical nonlinear dynamic instability of structures under seismic actions was given by the authors, and three practical criteria for determination of dynamic instability, i.e. criterion based on displacement, criteria based on tangent stiffness matrix, and criterion based on general stiffness parameter (GSP), were proposed as well (Li, 1998). The tests were carried out for the purposes as follows:

(1) To observe the phenomenon of the dynamic instability of the reticulated shell models under earthquake loading.
(2) To compare the test results with the process of dynamic instability described by the definition given by the authors.
(3) To verify the practical criteria of determination of dynamic instability under seismic actions proposed by the authors.

3. Design of the tests

Model tests of two shallow reticulated shells were carried out. All the members are 20# seamless steel tubes with section of $\phi 16 \times 2.0$ mm. Masses were hung under seven internal joints by specially fabricated components (see Fig. 1). The joints can be divided into three classes: central joint (1#), another six internal

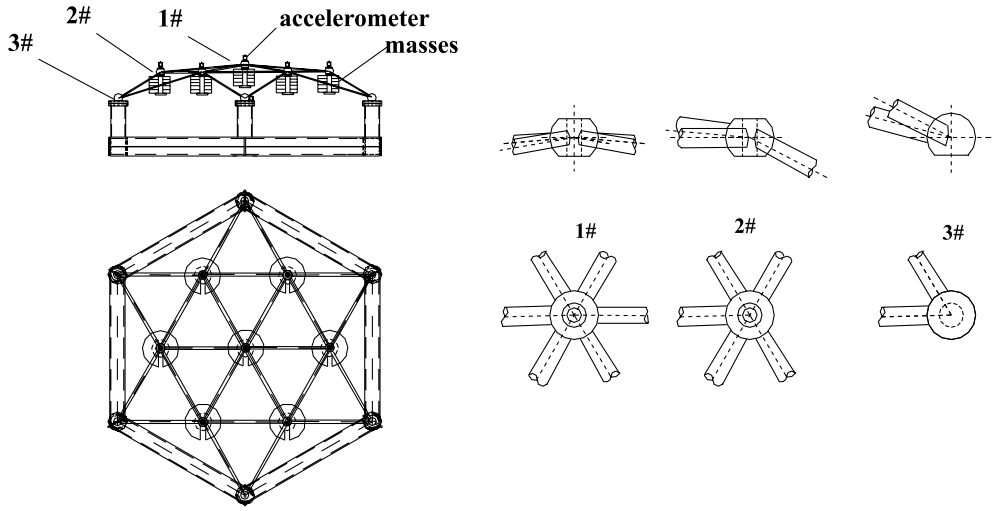

Fig. 1. Model assembling and detail of joints.

Table 1
Measured nodal coordinates of two models

Node	Model 1 (mm)			Model 2 (mm)		
	X	*Y*	*Z*	*X*	*Y*	*Z*
1	0.00	0.00	142.00	0.00	0.00	139.00
2	753.00	0.00	109.00	755.00	0.00	109.00
3	377.01	654.13	110.00	377.00	654.14	104.00
4	−380.49	654.43	109.00	−380.50	654.42	108.50
5	−758.00	1.15	110.00	−757.00	1.71	108.00
6	−380.48	−652.12	109.00	−377.48	−650.39	100.50
7	374.01	−652.40	110.00	377.00	−652.98	109.50
8	1300.49	757.46	0.00	1302.18	744.53	0.00
9	−0.91	1502.00	0.00	4.97	1501.99	0.00
10	−1300.84	748.87	0.00	−1303.57	754.15	0.00
11	−1299.35	−751.46	0.00	−1305.94	−748.02	0.00
12	2.64	−1497.00	0.00	−4.38	−1499.99	0.00
13	1301.99	−748.88	0.00	1300.98	−752.64	0.00

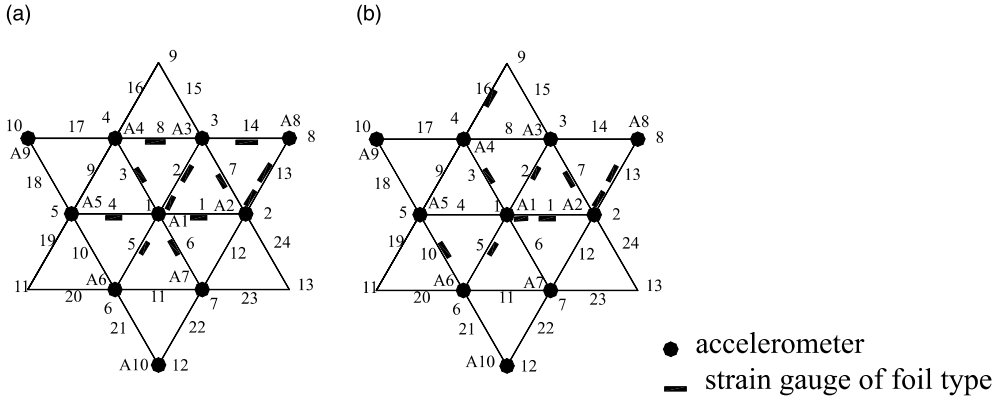

Fig. 2. Arrangement of accelerometers and strain gauges on two models.

joints (2#) and six peripheral joints (3#). The detail of joints is also given in Fig. 1. The measured nodal coordinates of two models are listed in Table 1.

Test points arranged on Model 1 and Model 2 are indicated in Fig. 2a and b. Accelerometers were fixed on part of the nodes. There were ten accelerometers on each model. Strain gauges of foil type were pasted on the upside and downside of the sections near the centers and the ends of members. There were 24 strain gauges on Model 1 and 20 strain gauges on Model 2 respectively.

Masses hung on the internal nodes of Model 1 and Model 2 are given in Table 2.

Mode 1 was subjected to a 0.7338 g scaled vertical El-Centro earthquake loading, and Mode 2 was first exerted a 0.4761 g and then a 0.6009 g scaled vertical El-Centro earthquake loading by the shaking table.

4. Experimental results of the two model tests

4.1. Test of Model 1

Under 0.7338 g scaled vertical El-Centro earthquake loading, global dynamic instability occurred at the time around the fifth second. The process of the dynamic instability can be described as follows: Node

Table 2
Masses hung on models' internal joints (unit: kg)

Node number	Model 1	Model 2
1	76.32	51.52
2	75.66	51.66
3	76.46	52.36
4	75.86	51.96
5	76.86	52.16
6	76.46	52.06
7	76.26	51.96

5 lost dynamic stability first, then Node 6, 1, 4 and 7, and finally the global dynamic instability was induced.

The time–history curves for vertical displacements of Node 1–Node 3 and Node 4–Node 7 of Model 1 are given in Fig. 3. All of the vertical displacements increased dramatically during dynamic instability. The displacements of Node 1–Node 7 also show that the changes of the time–history curves of all internal nodes were almost simultaneous when the model was in dynamic stable state, but near the critical point of dynamic instability, the vibrating characteristics of each node became quite different.

The time–history curves for dynamic stresses of the upside and downside of the sections at the center of Member 1 and 4 are given in Figs. 4 and 5 respectively. It is shown clearly that great changes took place during dynamic instability. This is due to the loss of partial or total structural capacity in the process of instability as the structures shifted from the initial vibrating state to a new one, which has higher structural

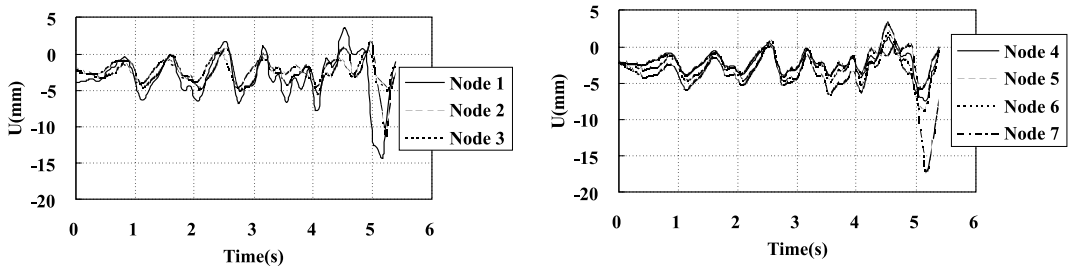

Fig. 3. Time–history curves for vertical displacement of Node 1–Node 7 of Model 1.

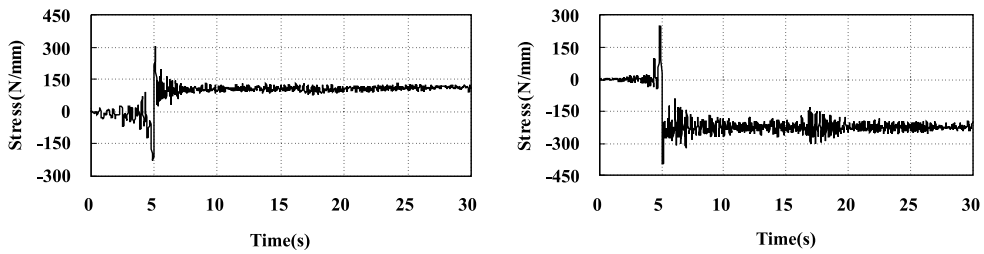

Fig. 4. Time–history curves for stresses of Member 1 in Model 1.

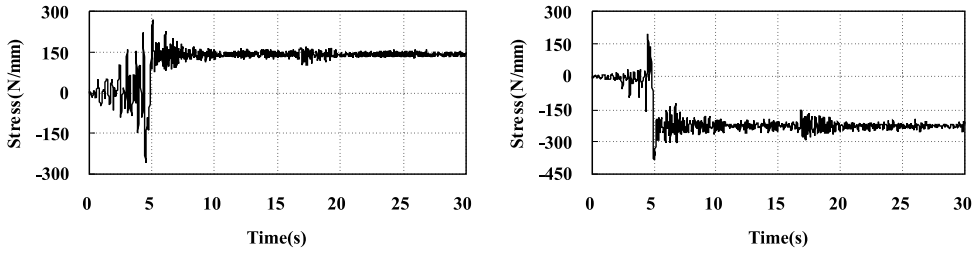

Fig. 5. Time–history curves for stresses of Member 4 in Model 1.

capacity and can keep a new stable vibrating state. The great change of time–history curves for stresses can be regarded as a sign of dynamic instability. Most members were in the elastic state before dynamic instability and changed into the elasto-plastic state when instability occurred.

4.2. Test of Model 2

When Model 2 was subjected to the 0.4761 g scaled vertical El-Centro earthquake loading, the local dynamic instability was observed at Node 5 near the sixth second and the model still kept global dynamic stability afterwards.

The time–history curves for vertical displacements of Node 1–Node 3 and Node 4–Node 7 of Model 2 are given in Fig. 6. It also can be seen that near the sixth second (about 5.6th second) the displacements of all internal nodes increased sharply. This was induced by local dynamic instability of Node 6.

The stress time–history curves of the upside and downside of the section at the center of Member 2 are given in Fig. 7. It is also shown that the stresses had changed dramatically near sixth second due to the local dynamic instability of Model 2.

After the 0.4761 g scaled earthquake loading, Model 2 was exerted another 0.6009 g scaled vertical El-Centro earthquake loading. The local dynamic instability occurred again near the sixth second at Node 6 and then the dynamic instability of Node 1 and Node 3 occurred in succession, which at last led Model 2 to be global dynamic instability near the 24th second (see Fig. 8).

The time–history curves for dynamic stresses of the upside and downside of the sections at the centers of Member 2 and 13 are given in Figs. 9 and 10 respectively. There were sudden changes in these time–history curves when Model 2 lost its global stability. The curves shifted from the last vibrating state to new ones.

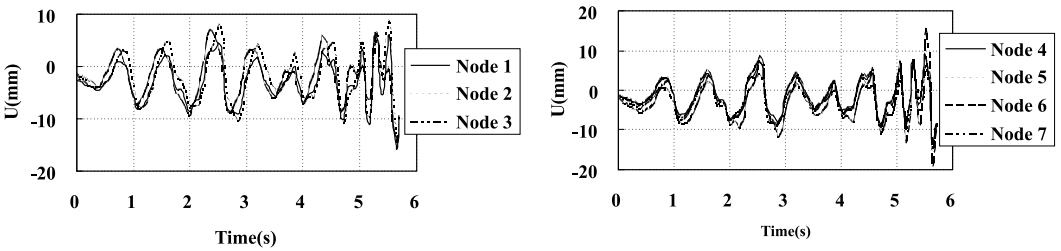

Fig. 6. Time–history curves for vertical displacements of Node 1–Node 7 of Model 2.

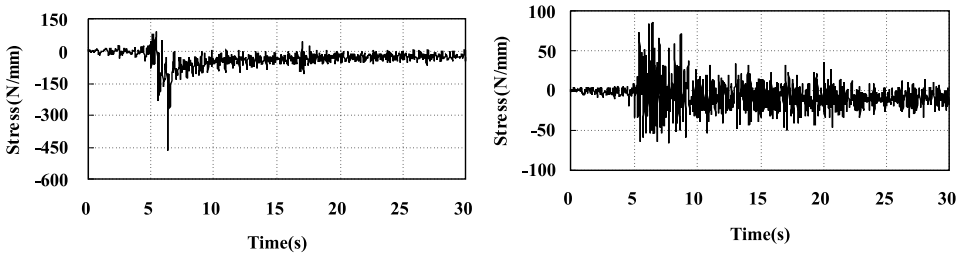

Fig. 7. Time–history curves for dynamic stresses of Member 2 in Model 2.

Fig. 8. Photo of global dynamic instability of Model 2.

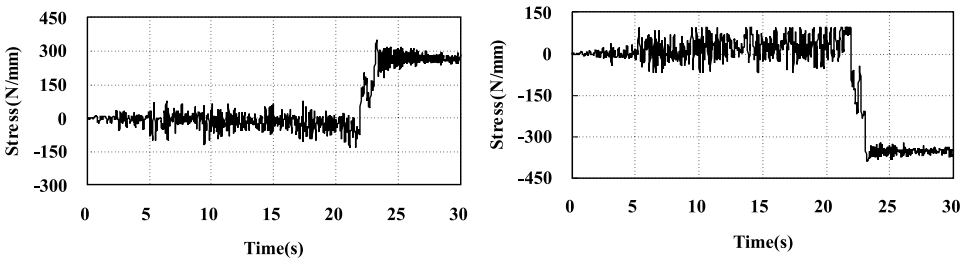

Fig. 9. Time–history curves for stresses of Member 2 in Model 2.

5. Main points drawn from the experiment

The experimental results and the phenomena observed in the test during the process of the dynamic instability of the models have sufficiently embodied the definition of elastic geometrical nonlinear dynamic instability of structures under seismic actions given by the authors (Li, 1998). The definition says that the

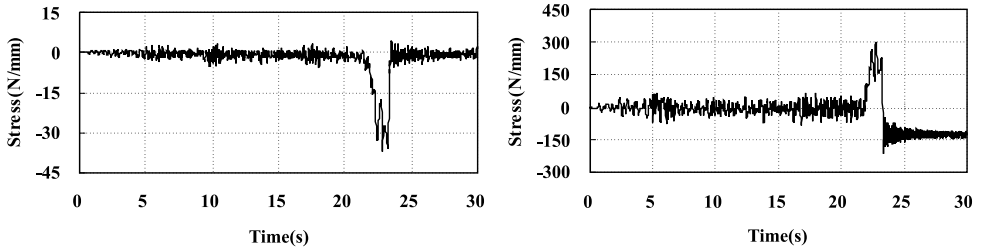

Fig. 10. Time–history curves for stresses of Member 13 in Model 2.

structural dynamic instability happens when the structural tangent stiffness matrix becomes nonpositive, which leads to the structural capacity decreasing or being lost locally or globally and results in the dynamic response of nodal displacements and structural deformation increasing dramatically. The definition also indicates that a structure when it is dynamic unstable at certain time may be stable afterwards due to the cycling behavior of the seismic action. In such case it is appropriate to say that the structural dynamic instability has occurred once. From this point of view, dynamic instability may occur several times for a same structure.

For verifying the practical criteria of determination of dynamic instability proposed by the authors, the static instabilities of two models were calculated. In calculation the ratio of the nodal loads vertically applied to the nodes is the same as the ratio of nodal masses of the two models.

The calculation results of the critical loads and displacements are as follows: for Model 1, the critical load of Node 1 is 1678.42 N, and the critical vertical displacement of Node 1 is 14.087 mm; For Model 2, the critical load is 1528.79 N and displacement is 10.324 mm. The curves of the static equilibrium paths and the GSP vs vertical displacements of Node 1 of the two models are shown in Fig. 11. These curves are calculated by using general displacement control method for static stability problems (Yang and Shieh, 1990). In Fig. 11, $F(N)$ is the resultant of vertical resistance of Node 1. It is shown that the structural capacity decreases or is lost in the process of instability, the GSP decreases with the deterioration of the structural stiffness, and is close to zero or becomes negative for one time when the equilibrium goes over the critical point. From Fig. 11, it can also be seen that the curves are different between the two models although the ideal geometry of them are the same, this demonstrates that the effects of the initial geometrical imperfections on structural stability are great.

The curves of the equilibrium paths and the GSP vs vertical displacements of Node 1 of the two models in the process of dynamic instability are given in Fig. 12. These curves are calculated using the improved general displacement control method suggested by the author (Li, 1998). It can be seen that there exist differences between the post-buckling equilibrium paths of static instability and dynamic instability.

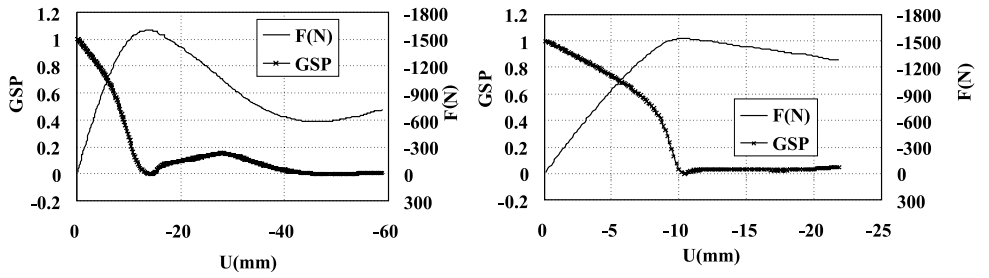

Fig. 11. Curves for vertical equilibrium paths and GSP vs vertical displacements of Node 1.

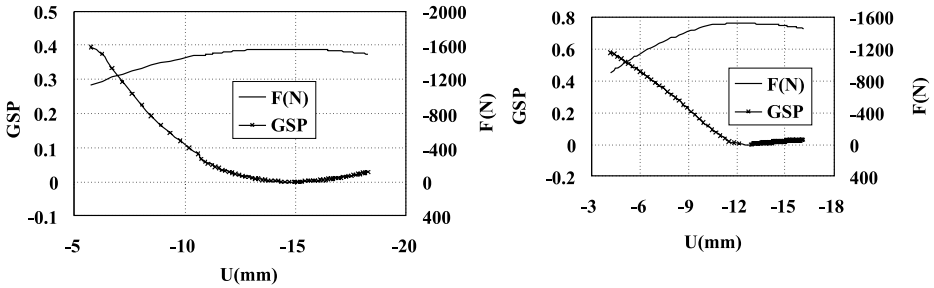

Fig. 12. Curves of vertical equilibrium paths and GSP vs vertical displacements of Node 1.

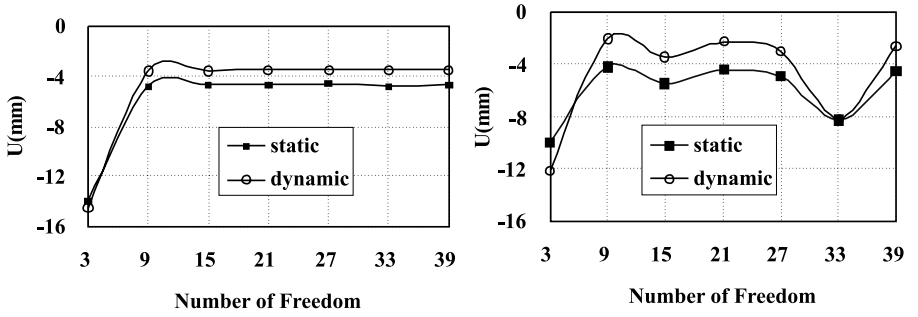

Fig. 13. Comparison between deformation modes of static stability and dynamic stability.

Comparison between the deformation modes of static stability and dynamic stability of Model 1 and Model 2 is given in Fig. 13, where the horizontal coordinates are the numbers of vertical freedoms of Node 1–Node 7 respectively, and the vertical coordinates are the related vertical displacements at critical points. It is shown that there are some differences between them.

From Figs. 11 and 12, the resultant of vertical resistance $F(N)$ and the vertical displacements of Node 1 during dynamic and static instability can be obtained and listed in Table 3.

Therefore, the comparison of Table 3 has verified the criterion based on displacement, i.e. the dynamic instability can be regarded as occurrence when the time–history curve of nodal displacement waves intensely in some time field and the amplitude overpasses the critical value of nodal displacement obtained from the elastic instability analysis under the same loading form (for dynamic problems, it means the equivalent dynamic force vector). This criterion can be used to estimate structural dynamic instability approximately.

In Fig. 12, it is shown that the resultant of vertical resistance $F(N)$ decreased after the occurrence of dynamic instability. This phenomenon indicates that the structural tangent stiffness matrix became non-

Table 3
Comparison between the results of dynamic stability and static stability

	Dynamic instability		Static instability	
	Critical load (N)	Displacement (mm)	Critical load (N)	Displacement (mm)
Model 1	1551.12	14.536	1678.42	14.087
Model 2	1525.18	12.167	1528.79	10.324

positive. All of these verified the criterion based on the tangent stiffness matrix, i.e. the structural dynamic instability happens when the structural tangent matrix becomes nonpositive.

In Fig. 12, it is also shown that GSP decreases with the increase of displacement, and its value goes down to zero at the time near the critical point and becomes negative for one time when the equilibrium path goes over the critical point. This phenomena verified the criterion based on GSP, i.e. the structural dynamic instability happens when GSP equals to zero or becomes negative.

6. Conclusions

Conclusions can be drawn from above testing results that the definition of dynamic instability, the criteria given by the authors are reasonable and practical. For large span space structures such as reticulated shells, once dynamic instability occurs, large deformation will occur in a short time, and the internal forces of structural members will increase rapidly. This will lead to losing serviceable function of structures and great catastrophe of economic loss and heavy casualty.

Acknowledgements

This work is supported by National Natural Science Foundation and State Key Laboratory for Disaster Reduction in Civil Engineering, the authors thank for their financial supports.

References

Blandford, G.E., 1996. Large deformation analysis of inelastic space truss structures. Journal of Structural Engineering, ASCE 122 (4), 407–415.

Blandford, G.E., 1997. Review of progressive failure analyses for truss structures. Journal of Structural Engineering, ASCE 123 (2), 122–129.

Fathelbab, F.A., 1987. The effect of joints on the stability of shallow single layer lattice domes. Ph.D. Thesis, University of Cambridge.

Gioncu, V., 1995. Buckling of reticulated shells: state-of-the-art. International Journal of Space Structures 10 (1), 1–46.

Hatzis, D., 1987. The influence of imperfections on the behavior of shallow single-layer lattice domes. Ph.D. Thesis, University of Cambridge.

Ikeda, K., Mahin, S.A., 1984. A refined physical theory model for predicting the seismic behavior of braced steel frames. Report No. UCB/EERC-84/12, Earthquake Engineering. University of California, Berkeley, CA.

Ishikawa, K., Kato, S., 1997. Elastic–plastic dynamic buckling analysis of reticular domes subjected to earthquake motion. International Journal of Space Structures 12 (3,4), 205–215.

Kato, S., Ueki, T., Mukaiyama, Y., 1997. Study of dynamic collapse of single layer reticular domes subjected to earthquake motion and the estimation of statically equivalent seismic forces. International Journal of Space Structures 12 (3,4), 191–203.

Kato, S., Mukaiyama, Y., 1995. Study on dynamic behavior and collapse acceleration of single layer reticular domes subjected to horizontal and vertical earthquake motions. Journal of Structural and Construction Engineering 77 (4), 87–96.

Kim, S.D., Kang, M.M., Kwun, T.J., 1997. Dynamic instability of shell-like shallow trusses considering damping. Computers and Structures 64, 481–489.

Li, Y.Q., 1998. Stability research on large span arch-supported reticulated shell. Ph.D., Tongji University.

Li, Z.X., 1998. Nonlinear dynamic stability analysis of steel lattice structures. Ph.D. Thesis, Tongji University.

Lightfoot, E., Le Messurier, A.P., 1974. Elastic analysis of frameworks with elastic connections. Journal of Structural Division, ASCE 100 (6), 1297–1309.

Meek, J.L., Loganathan, S., 1989. Theoretical and experimental investigation of a shallow geodesic dome. International Journal of Space Structures 4 (2), 89–105.

Morris, N.F., 1991. Effect of imperfections on lattice shell. Journal of Structural Engineering, ASCE 117 (6), 1796–1814.

Oda, K., 1986. On the joint rigidity of a ball joint system. International Symposium on Membrane Structures and Space Frames, Osaka.

Soroushian, P., Alawa, M.S., 1990. Hysteretic modeling of steel structs: a refined physical theory approach. Journal of Structural Engineering, ASCE 116 (11), 2903–2916.

Yang, Y.B., Shieh, M.S., 1990. Solution method for nonlinear problems with multiple critical points. AIAA Journal 28 (12), 2110–2116.

Ye, J.H., 1995. Dynamic stability analysis of single layer reticulated shell structures. Ph.D. Thesis, Tongji University.

Dr. Li Zhongxue, male, born in 1970, a lecturer of Civil Engineering Department, Zhejiang University.

Shen Zuyan, male, born in 1934, a professor of Civil Engineering College, Tongji University.